

# Supplementary Information

Pu Wang, Timothy Hunter, Alexandre M. Bayen, Katja Schechtner & Marta C. González

## TABLE OF CONTENTS

### I. DATA

A. Mobile Phone Data and Census Tract Data 2

B. Road Network Data 4

### II. METHOD

A. Estimation of the Transient OD for Vehicle Users 6

B. Incremental Traffic Assignment 15

C. Estimation of Travel Time from GPS Probe Data 16

D. Validation 20

### III. RESULTS

A. Supplementary Results 22

B. Statistical Analysis 27

REFERENCES 29

# I. DATA

## A. Mobile Phone Data and Census Tract Data

This section describes the data used in the main article. To this day these are the most extensive data sets which have been used to perform road usage studies. The San Francisco Bay Area mobile phone data are collected by a US mobile phone operator and contain about half a million customers. Each time a person uses a phone (call/text message/web browsing) the time and the mobile phone tower providing the service is recorded. This altogether generates 374 million location records in the three week observational period. A voronoi tessellation is used to estimate the service area of a mobile phone tower (1, 2). It provides the rough region where a mobile phone user can be located by his/her phone usage (Fig. S1A). The voronoi polygons located at the border are reshaped along the outline border of the San Francisco Bay Area census tracts to guarantee that they have reasonable service areas (Fig. S1A). Among these half a million users, we select 356,670 users to study the travel demands of the Bay Area residents (Table S1).

Properties:	Bay Area	Boston Area
Population	5,434,155	3,528,930
Area (mile <sup>2</sup> )	3,746	1,825
Population Density (/mile <sup>2</sup> )	1,451	1,934
Avg. Car Pool Size (people per car)	2.25	2.16
Mobile Phone Users	356,670	683,001
Total Length of Road Segments (miles)	15558.4	10346.5
Total Length of Road Segments/Population (miles/person)	0.00286	0.00293
Number of Arterial Roads	21,267	20,638
Number of Highways (Including Freeways)	3,141	1,267

**Table S1.** General information extracted from mobile phone data, census tract data and GIS data. The selected mobile phone users represent 6.56% and 19.35% of the population in the two metropolitan areas respectively. This is roughly two orders of magnitude larger in terms of population and time of observation than the most recent surveys (3). The length of road segments takes into account the num of lanes of a road segment.

In the Boston Area the coordinates of the recorded locations are estimated by a standard triangulation algorithm (location data do not come with tower ID). In the three weeks' observational

period, more than 200,000 distinct locations are recorded, this data is aggregated at the census tract level to define the location of a phone user (Fig. S1D). Consequently, we select 683,001 users from the one million mobile phone users in the Boston Area.

In both areas the selected mobile phone users have at least one location recorded between 9:00pm to 7:00am, allowing for the definition of home location in connection with a tower's service area or a census tract. The mobile phone users' home locations are also defined as the *driver sources*. We further find that a large majority of driver sources are located within dense mobile phone grids or small enough census tracts, thus providing accurate spatial resolution for the purpose of this study. The area distributions of driver sources are illustrated in Fig. S1B and E, and the respective density of population in Fig. S1C and F.

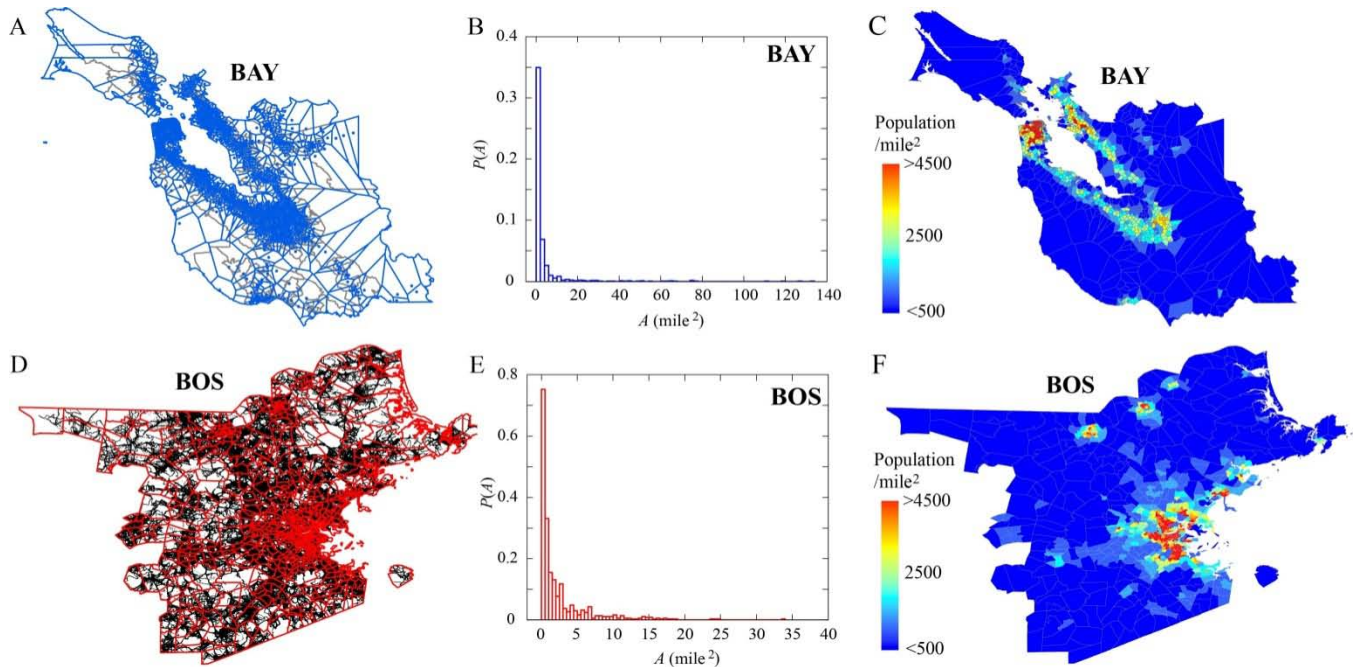


**Figure S1.** Location data and driver sources. (A) In the Bay Area (BAY), 892 mobile phone towers (blue dots) are used by the carrier. The covering areas of the towers are defined by a voronoi tessellation (blue polygons). The census tracts are represented by the light grey polygons. (B) The area distribution of Bay Area driver sources  $P(A)$  quantifies the probability that a driver source has an area  $A$ . The areas of most driver sources are small, indicating a high accuracy of driver sources' locations. (C) In the Bay Area, the population density of each driver source is calculated by the population of its overlapping census tracts. (D) In the Boston Area (BOS) driver sources are defined by census tracts (red polygons,

750 in total). Mobile phone users' coordinates are estimated by a standard triangulation algorithm, which results in more than 200,000 distinct locations with a 100m×100m spatial resolution (black dots). (E) Same with (B) for the Boston Area. (F) The population density in a Boston Area driver source is derived from the census tract data.

As shown in Fig. S2, we measure the population in each driver source. Since mobile phone towers and census tracts are designed to serve similar number of population, we find that driver sources have a similar order of magnitude.

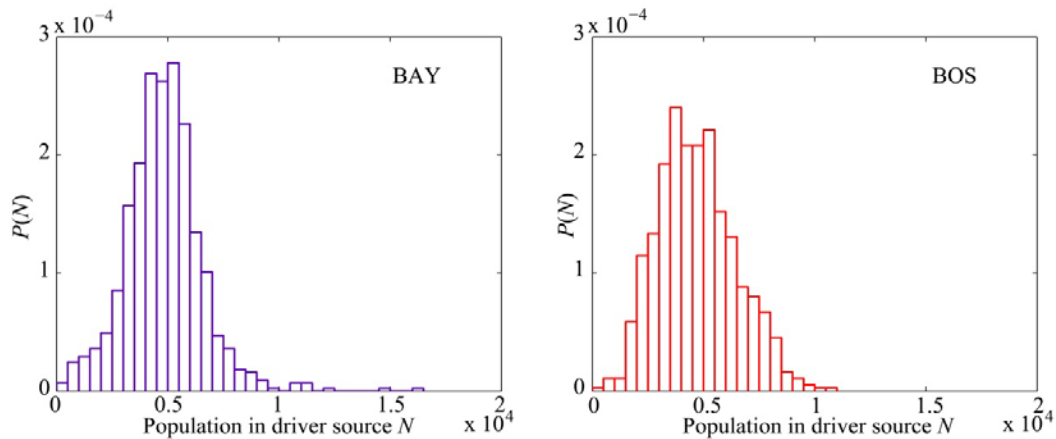


**Figure S2.** The distribution of population in driver sources.  $N$  is the population of a driver source. In the Bay Area, a driver source is a mobile phone tower's service area. In the Boston Area, a driver source is a census tract.

Users' privacy is protected by using anonymized user IDs. In addition, the spatial resolution of the voronoi lattice or the census tract provides sufficiently large areas to prevent personal location identification at an individual level. Furthermore, no individual trajectory is shown in our results.

## **B. Road Network Data**

The road networks, which include both highways and arterial roads, are provided by NAVTEQ, a commercial provider of geographical information systems data (4). The data incorporate the attributes of roads needed for the computations presented in this work, in particular the road capacity. The road

network in the Bay Area contains 21,880 road segments and 11,096 intersections, while the road network in the Boston Area contains 21,905 road segments and 9,643 intersections. For each road segment, the speed limit  $sl$  (miles/hr), the number of lanes  $l$  and the direction are extracted from the database. According to 2000 Highway Capacity Manual (5) and Reference (6), we estimate the capacity  $C$  of a road segment as follows:

- (1) when the speed limit of a road segment  $sl \leq 45$ , it is defined as an arterial road:

$$C = 1,900 \times l \times q \text{ (vehicles/hour)} \tag{S1}$$

for simplicity, the effective green time-to-cycle length ratio  $q$  is selected to be 0.5.

- (2) when the speed limit of a road segment  $45 < sl < 60$ , it is defined as a highway:

$$C = (1,000 + 20 \times sl) \times l \text{ (vehicles/hour)} \tag{S2}$$

- (3) when the speed limit of a road segment  $sl \geq 60$ , it is defined as a freeway:

$$C = (1,700 + 10 \times sl) \times l \text{ (vehicles/hour)} \tag{S3}$$

In Fig. S3, we show the distribution of road segment lengths. We find similar distributions in Bay Area and Boston Area, albeit the detected maximum length is larger in the Bay Area.

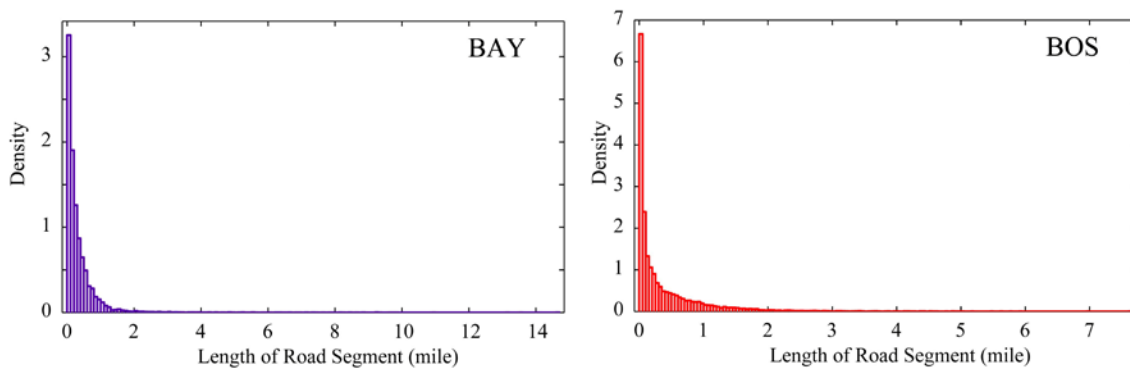


**Figure S3.** The distribution of road segment lengths.

## II. METHOD

### A. Estimation of the Transient OD for Vehicle Users

#### *1. Introduction:*

The Origin-Destination matrices (OD) provide information on flows of vehicles travelling from one specific geographical area to another and serve as one of the critical data inputs for transportation planning, design and operations (7). Currently OD is usually estimated from household interviews or incomplete traffic counts (8, 9). Traditional census and household interviews data fail to generate detailed and updated travel demands due to the high cost and low accuracy coupled with this method (8, 9). Road cameras and loop detectors can record the number of vehicles passing by, yet they are expensive to install and prone to errors and malfunctioning (8, 9), and consequently mostly limited to highways and freeways (8, 9). GPS data (10) collects location traces of probe vehicles at high resolutions (up to one Hz), yet they are not ubiquitous and fail to provide full OD information at a large scale. Furthermore, due to privacy issues they are often degraded on purpose (leading to down sampling of data), and thus insufficient as a standalone data source. Mobile phone data on the other hand, offer enormous amounts of location information, providing us with an opportunity to improve the estimation of the OD economically (11). An inherent advantage of mobile phone data comes from their wide availability. Because of the generic format of mobile phone data, any methodology relying on their analysis can easily be applied to other locations for which GIS data are also available, thus providing a unique framework pertinent to a variety of problems.

#### *2. Definition of trips and extraction of travel demands:*

The major challenge when estimating travel demands with mobile phone data is embedded in the sparse and irregular records (12), in which user displacements (consecutive different recorded locations) are usually observed between a long period (i.e. the first location is observed at 8:00am and next

location is observed at 6:00pm). To more accurately extract users' travel demands between zones (mobile phone towers' service areas for the Bay Area and the census tracts for the Boston Area), we only record displacements occurring within a short time window. However, the time window we select must be long enough in order to ensure that enough travel demand information is extracted. In our modelling framework, we set the time window to one hour and define a *trip* as a displacement occurring within one hour in each time period (i.e. Morning Period, Noon & Afternoon Period, etc). Fig. S4 illustrates a mobile user's time and location records, using the presented approach; in this example two trips are detected.

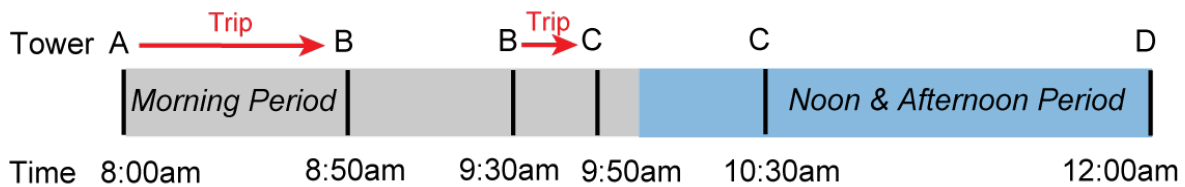


**Figure S4.** Illustration of trip definition from a mobile phone user's billing record. Black lines represent phone usage records, for each of them the time and the associated towers (A-D) routing the service are recorded. Changes of locations C->D are not defined as a trip, because they do not occur within a one-hour time window. Two trips are detected: from 8:00am tower A to 8:50am tower B and from 9:30am tower B to 9:50am tower C.

### 3. Definition of transient OD:

In the mobile phone data, a user's location information is lost when he/she does not use his/her phone. As Fig. S5 shows, a user is observed to move from zone B to zone C (he/she has calls or text messages in zone B and zone C), but his/her initial origin (O) and final destination (D) may actually be located in zone A and zone D. Thus, in such cases we lose a segment of the trip information (denoted by the dashed blue lines). Even if we only capture the transient origin and destination with the phones, this still allows us to capture a large portion of the road usage. Thus, we put forward the transient origin destination (*t*-OD) matrix, which requires only mobile phone data as input, to efficiently and economically capture the detailed travel demand information.

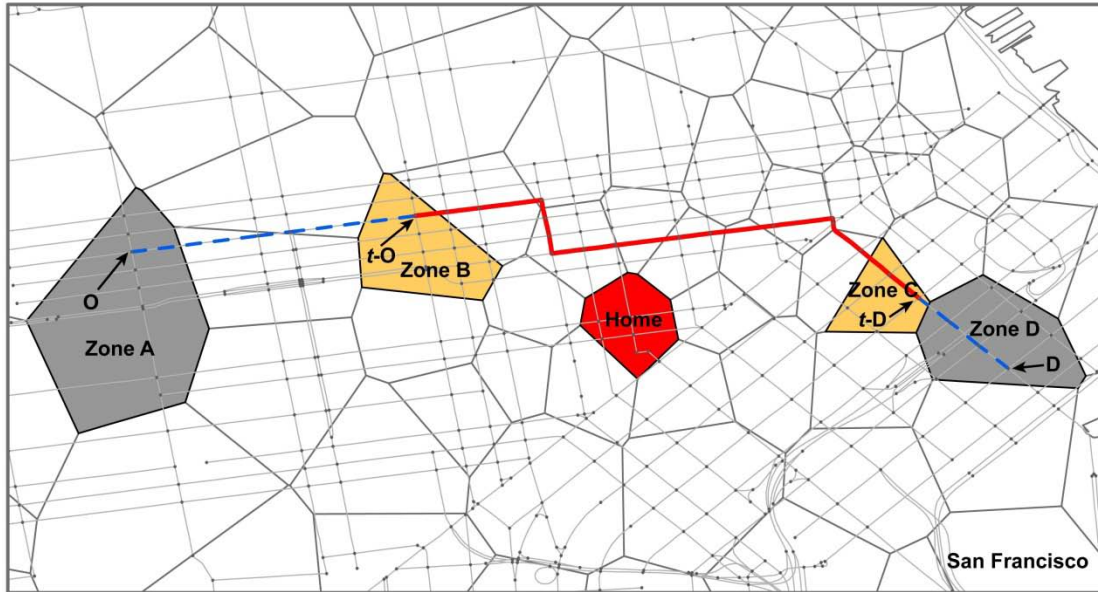


**Figure S5.** Illustration of a mobile phone user’s OD,  $t$ -OD and home location. The road segments in the vicinity of San Francisco downtown are depicted by grey lines and the small black dots are the road intersections that lie in the zones (mobile phone towers’ service areas). A driver drives from zone A (origin) to zone D (destination), however, he/she may only be detected by phone records at zone B (transient origin) and zone C (transient destination). The thick red line is the predicted route from the observed  $t$ -OD, whereas the dashed blue line represents the missing segment of the route. The driver’s home location (driver source) is highlighted in red.

#### 4. *Generation of travel demands independent of the frequency of phone activity:*

Obviously, users with more calls (text messages/web browsing) have more trips being extracted by the presented method. So one question arises: will this introduce bias to calculate the distribution of travel demands? To answer this question, we first measure the number of transactions (call/text message/web browsing) for the Bay Area and Boston Area users. As Fig. S6A shows, we find very similar distributions in the two areas. Thus, we use the same criterion to divide the mobile phone users into five groups, labelled I to V. The users in group I have less than 10 transactions, representing less than 5% of the user base. Group II, III, IV include the users with 10-500 transactions, 500-1,000 transactions and 1,000-2,000 transactions respectively, which overall represent ~90% of the selected users in the two areas. The mobile phone users in group V are extremely heavy users who have more than 2,000 transactions.



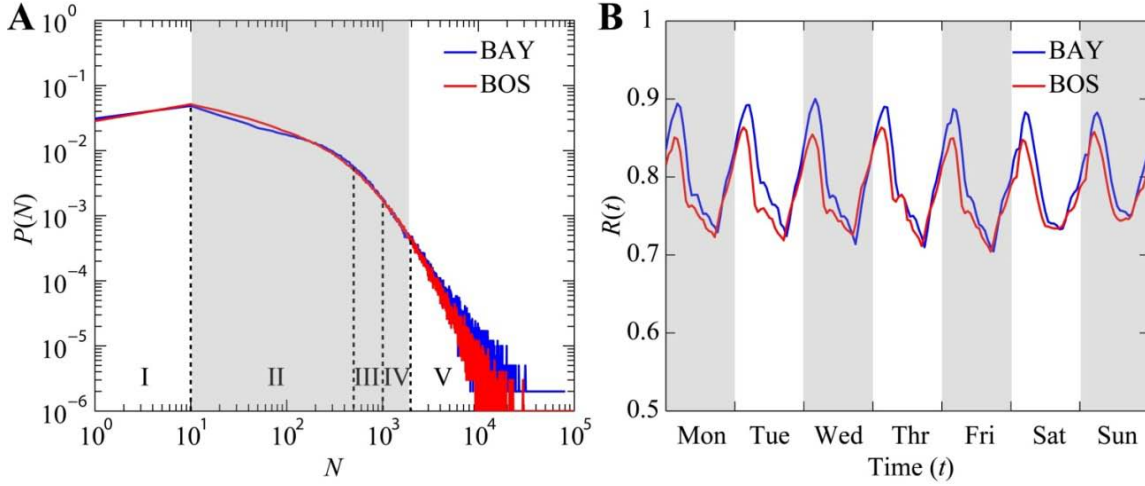


**Figure S6.** (A) The distribution of the number of transactions.  $P(N)$  is the probability that a mobile phone user has  $N$  transactions in three-week long observational period. Users are divided into five groups by the dashed lines and the users in group II, III and IV (the shaded area with grey colour) are used to extract trips between zones. (B) The hourly regularity  $R(t)$  over a week-long period. It measures the probability when the user is found in his or her most visited location during the corresponding hour-long period.

We next count the number of trips  $F_{ij}$  between zone  $i$  and zone  $j$  in a specific time period:

$$F_{ij} = \sum_{n=1}^N T_{ij}(n) \quad (\text{S4})$$

where  $N$  is the total number of selected users and  $T_{ij}(n)$  is the total number of trips that user  $n$  made between zone  $i$  and zone  $j$  in the observational period. The number of trips between zones  $i$  and zone  $j$  is then normalized by the total number of trips  $\sum_{i,j} F_{ij}$  between all zones to obtain the distribution of travel demand  $P_{ij}$ :

$$P_{ij} = F_{ij} / \sum_{i,j} F_{ij} \quad (\text{S5})$$

To test if  $P_{ij}$  is sensitive to the selection of light or heavy users, we calculate  $P_{ij}$  for users in group II, III, IV and V respectively (we do not use group I users, because they have too few locations recorded). We find that the  $P_{ij}$  calculated from users in group II, III and IV are highly correlated (Pearson correlation coefficient  $PCC > 0.93$ , Fig. S7), indicating that the distribution of travel demands is not

sensitive to the selection of light or heavy users within a broad range. We find only a low  $PCC$  between users in groups II and V, consequently we do not take the small group of extremely heavy users (group V) into account. Thus we employ data from the user groups II, III and IV in our simulation.

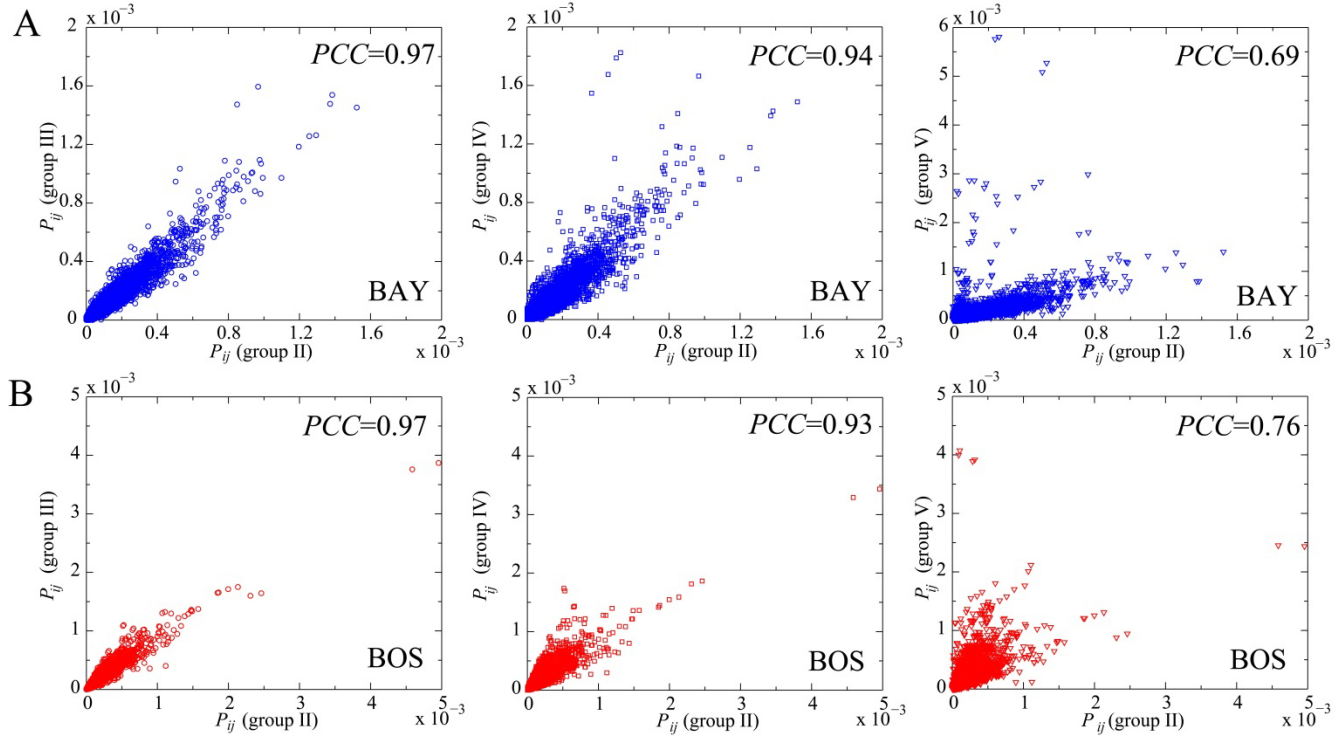


**Figure S7.** The distribution  $P_{ij}$  of travel demands extracted from users in group II, III, IV and V. **(A)** In the Bay Area (BAY),  $P_{ij}$  is extracted from group II, III, IV and V users respectively. The  $P_{ij}$  extracted from users in groups II, III and IV are highly correlated, whereas a lower correlation is found between the  $P_{ij}$  from group II and V users. To avoid the bias caused by these extremely active users, we employ users from group II, III and IV (91.5% of the selected 356,670 users) to extract the travel demand distribution. **(B)** Same as (A) but for the Boston Area (BOS) with 89.5% of the selected 683,001 users.

### 5. Generating the vehicle based transient OD:

One may note that the extracted distribution of travel demands did not take the population distribution into account. To avoid the bias caused by the unevenly distributed mobile phone user market share, we define the down-scale ratio ( $M(i) < 1$ ) or the up-scale ratio ( $M(i) \geq 1$ ) as follows:

$$M(i) = N_{pop}(i)/N_{user}(i) \quad (S6)$$

where  $N_{pop}(i)$  and  $N_{user}(i)$  are the population and the number of selected mobile phone users in zone  $i$ . The measured  $M(i)$  distributions are shown in Fig. S8. For both areas, they are relatively broad, thus it is necessary to adjust the number of trips  $F_{ij}$  by up-scaling or down-scaling the mobile phone users (Eq. S7).

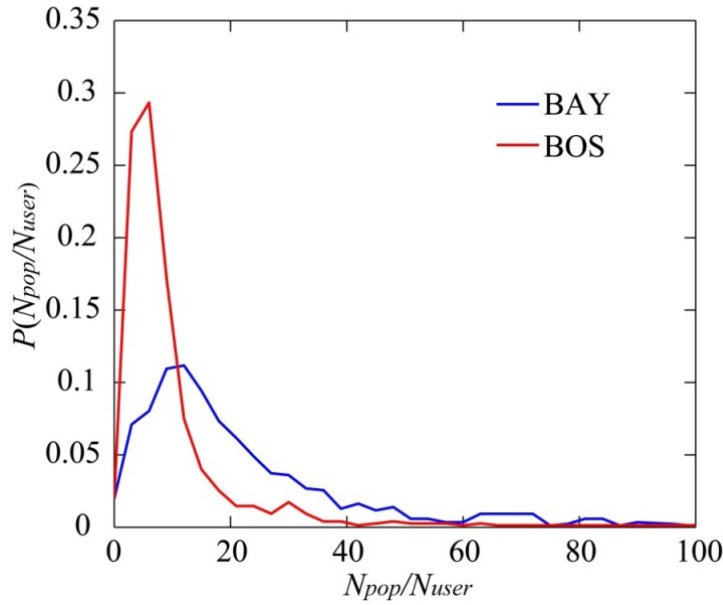


**Figure S8.** The blue curve corresponds to the distribution of up-scaling/down-scaling ratios  $N_{pop}/N_{user}$  in the Bay Area (BAY) zones. The red curve corresponds to that in the Boston Area (BOS) zones. Note that in some regions the actual number of mobile phone users staying there may be larger than the number of residents registered by census.

After this process, the total number of trips generated by residents in a zone is proportional with its actual population:

$$F_{ij}^{all} = \sum_{n=1}^{N_k} T_{ij}(n) \times M(k) \quad (S7)$$

where  $N_k$  is the total number of users in the  $k^{th}$  zone and  $T_{ij}(n)$  is the total number of trips that user  $n$  made between zone  $i$  and zone  $j$  during the three weeks of study.

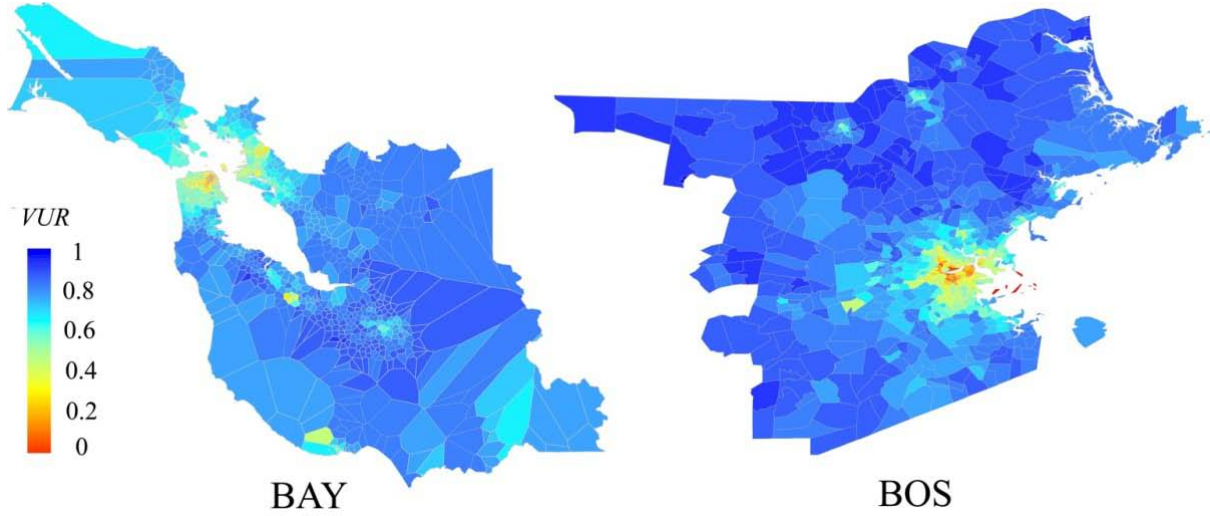


**Figure S9.** Vehicle usage rates by geographical area. Different colours represent different vehicle usage rates ( $VUR$ ). Urban areas have lower  $VUR$  than suburban areas, as can be noticed for San Francisco, a part of the east Bay and Santa Cruz, as well as for Boston.

People use different transportation modes throughout their trips. Possible transportation modes include car (drive alone), carpool, public transportation, bicycle and walk. We define a user is a vehicle user if he/she uses car to commute. We calculate the vehicle using rate ( $VUR$ ) in a zone as follows:

$$VUR(i) = P_{car\ drive\ alone}(i) + P_{carpool}(i)/S \quad (S8)$$

where  $P_{car\ driver\ alone}(i)$  and  $P_{car\ pool}(i)$  are the probabilities that residents in zone  $i$  drive alone or share a car. The average carpool size  $S$  is 2.25 in California and 2.16 in Massachusetts (13). As shown in Fig. S9,  $VUR$  is low in downtown and high in the suburb areas. Using the  $VUR$  calculated for each zone, we randomly assign the transportation mode (vehicle or non-vehicle) to the users living in each zone. We then filter the trips that are not made by vehicles and calculate the total number of trips generated by vehicles  $F^{vehicle}_{ij}$ :

$$F^{vehicle}_{ij} = \sum_{n=1}^{N_k} T_{ij}(n) \times M(k) \quad (S9)$$

where user  $n$  is a vehicle user,  $N_k$  is the number of users in zone  $k$ .

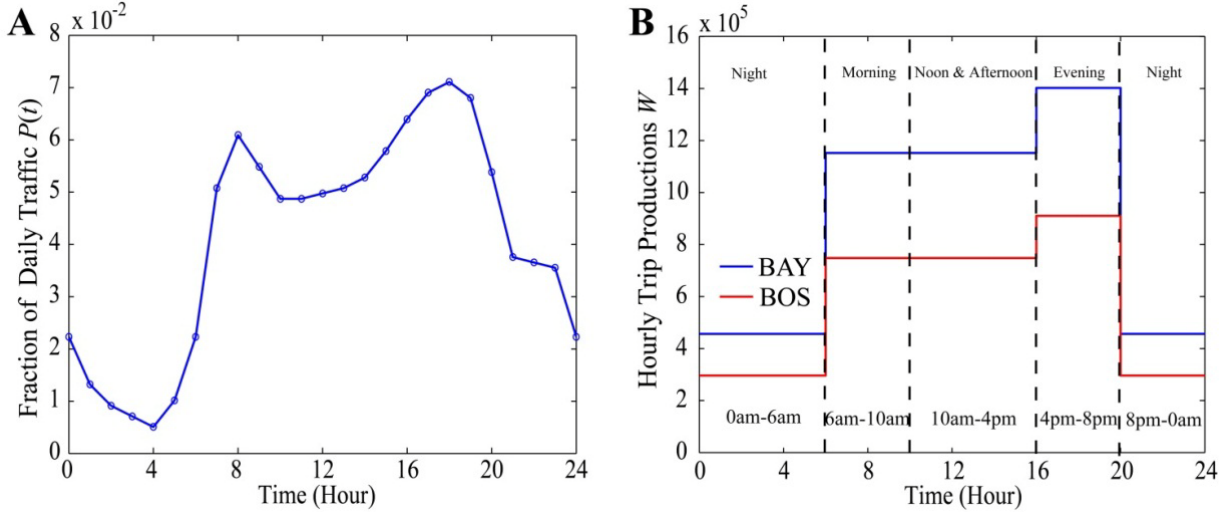


**Figure S10.** Distribution of daily traffic. **(A)** In each hour, the traffic contributed by vehicles represents a specific fraction of daily total traffic. **(B)** The average hourly total trip productions in the four time periods. For each time period, the hourly total trip productions are assigned as the average.

The average number of daily trips per person is about 4 in the US (14). This generates about 22 million trips in the Bay Area and 14 million trips in the Boston Area. Based on the daily distribution of traffic volume obtained from (15), we estimate the average hourly trip production  $W$  in the four time periods (Fig. S10B). Next, we upscale the obtained distribution of travel demands with the hourly trip production  $W$  for the entire population, thus finally defining the estimated  $t$ -OD.

$$t\text{-OD}_{ij} = W \times \frac{F^{vehicle}_{ij}}{\sum_{ij}^A F^{all}_{ij}} \quad (\text{S10})$$

where  $A$  is the number of zones. The following flow chart summarizes the methodology to calculate  $t$ -OD (Fig. S11).

## Flow Chart for the Calculation of $t$ -OD

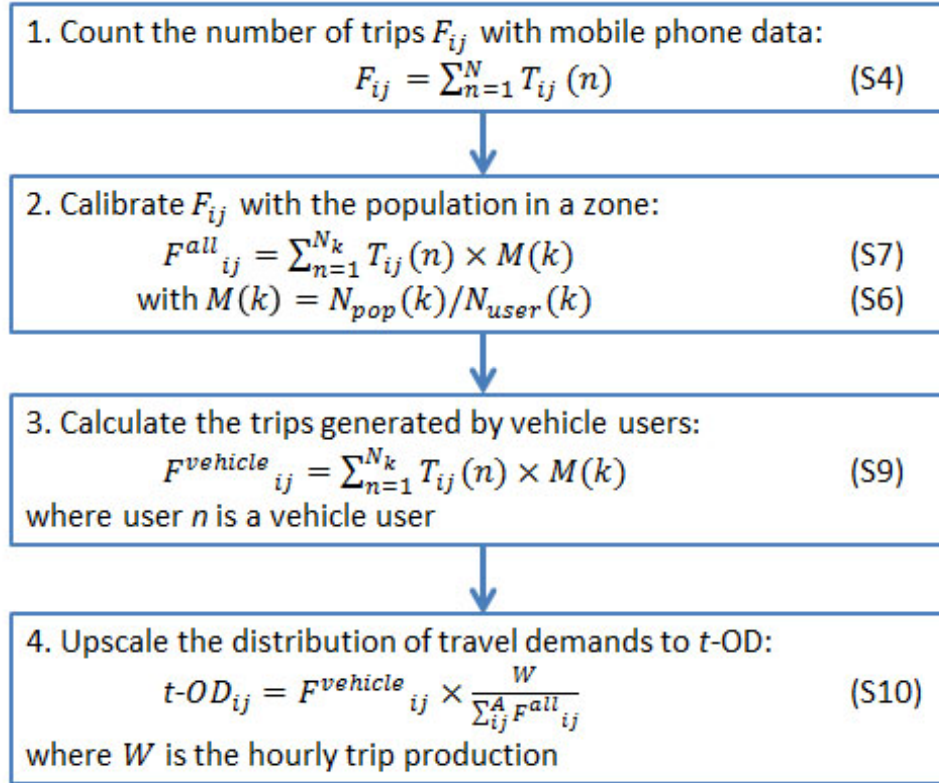


**Figure S11.** Flow chart for the calculation of  $t$ -OD.

### 6. *Converting zone based $t$ -OD to intersection based $t$ -OD:*

To assign trips to the road networks, we map each  $t$ -OD pair from zone based  $t$ -OD to intersection-based  $t$ -OD. We find the road intersections within a zone and randomly select one intersection to be the origin or destination in the intersection-based  $t$ -OD (Fig. S5). In very few cases no intersection is found in a zone. In such cases we assign a trip's origin or destination to a randomly chosen intersection in the nearest neighbouring zone. We generate four  $11,096 \times 11,096$  intersection based  $t$ -OD from the four  $892 \times 892$  zone based  $t$ -OD in the Bay Area (the Bay Area road network contains 11,096 intersections). For the Boston Area, we generate four  $9,643 \times 9,643$  intersection based  $t$ -OD from the four  $750 \times 750$  zone based  $t$ -OD (the Boston road network contains 9,643 intersections).

## B. Incremental Traffic Assignment

With the intersection based  $t$ -ODs calculated, we next assign the trips to the two road networks. The most fundamental method is provided by the classic Dijkstra algorithm, commonly used for routing in transportation networks (16). Dijkstra's algorithm is a graph search algorithm that solves the shortest path problem for a graph with nonnegative edge path costs (travel time in our case). With the Dijkstra algorithm, we can find the shortest path with minimum travel time between the origin and destination in a road network. However, the Dijkstra algorithm ignores the dynamical change of travel time in a road segment. Thus to incorporate the change of travel time, we apply the incremental traffic assignment (ITA) method (17) to assign the  $t$ -OD pairs to the road networks. In the ITA method, the original  $t$ -OD is first split into four sub  $t$ -ODs, which contain 40%, 30%, 20% and 10% of the original  $t$ -OD pairs respectively. These fractions are the commonly used values (18). The trips in the first sub  $t$ -OD are assigned using the free travel time  $t_f$  along the routes computed by Dijkstra's algorithm. After the first assignment, the actual travel time  $t_a$  in a road segment is assumed to follow the Bureau of Public Roads (BPR) function that widely used in civil engineering  $t_a = t_f(1 + \alpha(VOC)^\beta)$ , where commonly used values  $\alpha = 0.15$  and  $\beta = 4$  are selected (18). Next, the trips in the second sub  $t$ -OD are assigned using the updated travel time  $t_a$  along the routes computed by Dijkstra's algorithm. Iteratively, we assign all of the trips in the four sub  $t$ -ODs. In the process of finding the path to minimize the travel time, we record the route for each pair of transient origin and transient destination.

The advantages of the ITA method consist of two aspects. First, it takes the dynamical change of travel time into account, mimicking the process of drivers selecting routes according to their knowledge of the traffic in a road network. Indeed, traffic flows predicted by the ITA method are a very good approximation of those predicted by the widely used User Equilibrium traffic assignment (UE) method (19). We find high correlations between the traffic flows predicted by the ITA method and the UE method in Fig. S12, which motivates the use of the ITA method for our work (it can be implemented easily without suffering from the computational complexity of UE solutions). Second, another advantage

of the ITA method over the UE method is that by using the ITA method we can easily estimate the route of each OD pair, offering us the opportunity to study the road usage with respect to a road segment's driver sources (discussed in the main article).

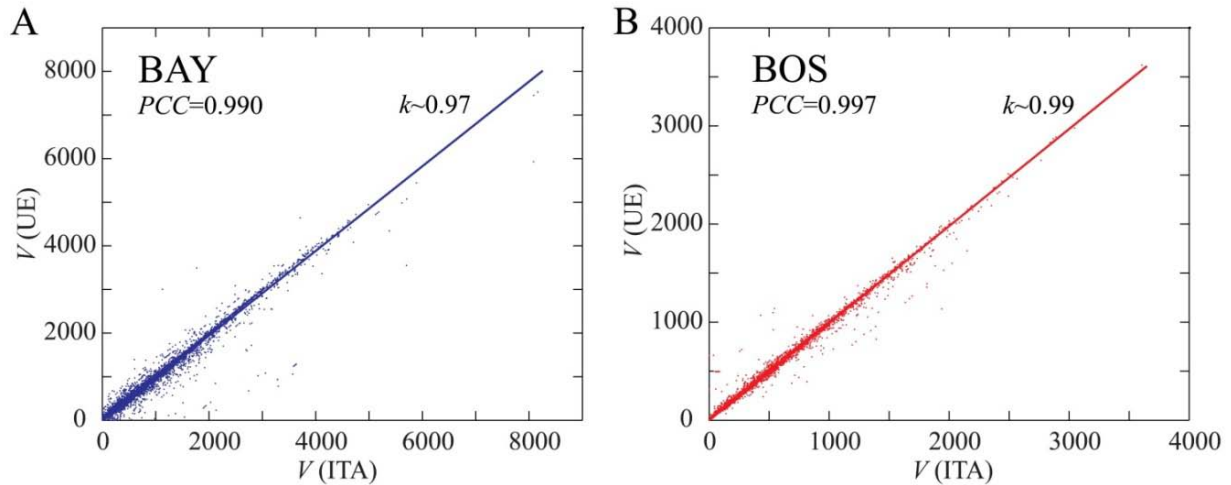


**Figure S12.** Validation of the ITA method. The x-axis represents the traffic flows (vehicles/hour) predicted by the ITA method and the y-axis represents that calculated by the UE method (UE function in TransCAD). The consistency of the results shows that the ITA method is a good approximation of the UE method. (A) shows the Bay Area (BAY). (B) shows the Boston Area (BOS).

### C. Estimation of Travel Time from GPS Probe Data

In order to validate the results from the previous sections, an independent data set is needed in order to compare the corresponding estimates with these independent measurements. Probe vehicle data based on GPS receivers has enjoyed a widespread use in transportation. However it must be said that it will not be possible in the near future to use GPS probe data to calculate traffic volumes in whole urban road networks. This is because the amount of probe data is still too low to be used for inference of traffic volumes. Probe data has successfully been used to compute travel times and speeds along freeways and arterials (20). Thus, the validation process used to assess the accuracy of our method will rely on travel



time and speed as a proxy, which we can infer from probe data provided by taxicabs and commercial vehicle companies.

This data show unique advantages for tracking a fleet of vehicles and routing and navigation. The receivers are usually attached to a car or a truck (referred to as a probe vehicle), and they relay information to a base station using the data channels of the cell phone networks. A datum provided by probe vehicles includes an identifier of the vehicle, a GPS position and a timestamp. In order to reduce power consumption and transmission costs, the probe vehicles do not continuously report their location to the base station. Instead they relay their position either at fixed times (every second to every minute), or at some landmark positions (a concept patented by Nokia under the term Virtual Trip Time) (21). This data type is very popular, especially amongst transportation companies for tracking purposes, but presents unique challenges for estimating traffic flows patterns:

- (1) The precise location of the vehicle is known with some error, due to GPS observation noise.
- (2) The path of the vehicle between two consecutive observations can be significantly long, and is usually unobserved.

The approach used in this work is to reconstruct the trajectories of the vehicles as accurately as possible, using machine learning techniques. From these trajectories, only sample points are observed, between which the travel time is known. This information (travel time, reconstructed trajectory) is then passed on to a second learning algorithm that learns travel times on every road link. This process is repeated for every day of the week and every 15 minutes of a day to calculate a weekly historical estimate of the traffic. We briefly describe the mapping algorithm below and then introduce the travel time learning algorithm (Fig. S13).

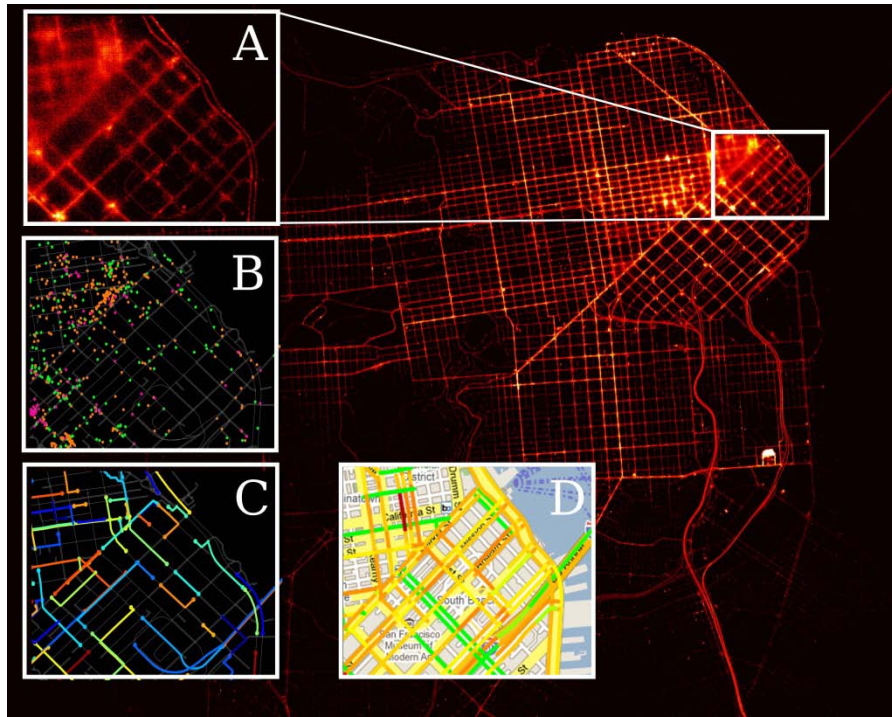


**Figure S13.** Estimation of travel times using probe vehicle data. In the background, the density map of probe data around San Francisco is shown. The maximum density (in white) corresponds to 7.2 GPS observations per hour and per square meter. **(A)** focuses on the Embarcadero neighborhood. **(B)** shows the GPS observations (sent every minute) collected from three vehicles in that area between 8am and 10am. The trajectory of each vehicle is reconstructed from the sequence of GPS points using the Path Inference algorithm. **(C)** presents a few trajectory segments between two consecutive GPS point. The EM algorithm then infers the travel times on each road link, by learning from these time-stamped segments. **(D)** shows a typical output of the travel time algorithm, at 8am on a Monday Morning.

### *Map Matching Algorithm*

The GPS error is assumed to follow a (nearly Gaussian) dispersion model. Meanwhile, the driver's behaviour on the road is assumed to follow a model that indicates the preferences of the driver between one path and another. Our framework can be decomposed into the following steps:

Map matching: each GPS measurement from the input is projected onto a set of candidate states on the road network. The vehicle is assumed to have been in either of these candidate states when the GPS observation was made.

Path discovery: a number of potential paths are computed between pairs of candidate states on the road network. The vehicle is assumed to have followed one of these paths when it travelled from the previous observation to the next

Filtering: probabilities are assigned to the paths and the states using a model of the driver's preferences and of the GPS dispersion. These probabilities are computed using a dynamic programming approach, using a probabilistic structure called a Conditional Random Field. Using the Viterbi algorithm, the most likely trajectory is obtained. At the output of the filter, we obtain reconstructed trajectories, along with time stamped waypoints. This dataset is then used to computing historical travel time estimates.

### ***Expectation Maximization Algorithm***

Each segment of the trajectory between two GPS points is referred to as an observation. An observation consists of a start time, an end time and a path on the road network. This path may span multiple road links, and starts and ends at some offset within some links. The observations are grouped into 15 minute time intervals and sent to a traffic estimation engine, which runs the learning algorithm described next and returns probability distributions of travel times for each link. The goal of the traffic estimation algorithm is to infer how congested the links are in a road network, given periodic GPS readings from vehicles moving through the network. An additional difficulty in estimating the travel time distributions is the lack of travel times for the individual links. Instead, each observation only specifies the total travel time for an entire list of links travelled. To solve this problem, we use an iterative expectation maximization (EM) algorithm. The central idea of the algorithm is to randomly partition the total travel time among links for each observation, and then weigh the partitions by their likelihood according to the current estimate of travel time distributions. Next, given the weighted travel time samples produced for each link, we update the travel time distribution parameters for the link to maximize the likelihood of these weighted samples. By iteratively repeating this process, the algorithm converges to a set of travel time distribution parameters that fit the data well. The sample generation

stage is called the expectation (E) step, and the parameter update stage is called the maximization (M) step. This procedure rapidly and reliably converges to some estimated travel times for every road of the network.

#### **D. Validation**

Due to the lack of reliable traffic flow data at a global scale (due to the insufficient volume of probe data), we compare for each road segment the predicted travel time with the average travel time calculated from the probe vehicle GPS data (the data is mostly obtained from Taxi fleets). According to the BPR function, the travel time of a road segment is decided by its traffic flow. A road segment's travel time increases with the increase of its traffic flow. Hence, obtaining the travel time from GPS probe data can be an indirect way to validate our results on the distribution of traffic flow. For 68% of the road segments in the Bay Area road network (16,594), the probe vehicle GPS data record the average travel time in each 15 minute interval of the one week observational period. Using this data, we calculate the average travel time for each road segment in the four time periods considered for this work (Morning, Noon & Afternoon, Evening and Night). We find that the predicted travel time from the  $t$ -OD has a good linear relation  $T_{\text{prediction}} = kT_{\text{probe vehicle}}$  with the average travel time estimated from the probe vehicle GPS data (the coefficient of determination  $R^2 > 0.9$  for all time periods). The Pearson correlation coefficients ( $PCC$ ) are larger than 0.95 for all time periods (Fig. S14). The slope  $k$  is about 0.75 in the daytime, which may be caused by the relatively frequent waiting or speed deceleration when drivers wait at traffic lights (we did not consider traffic signals in the presented modelling framework). The slope is about 1 in the Night period, indicating the high vehicle speeds during this period. Taken together we find a high correspondence between our predicted result and the GPS probe data estimation, demonstrating the strength of the presented methodology. Furthermore, elements such as more accurate information about road capacity, free travel time and parameters for the BPR function and traffic signals can be integrated into our fundamental modelling framework to enrich future predictions.

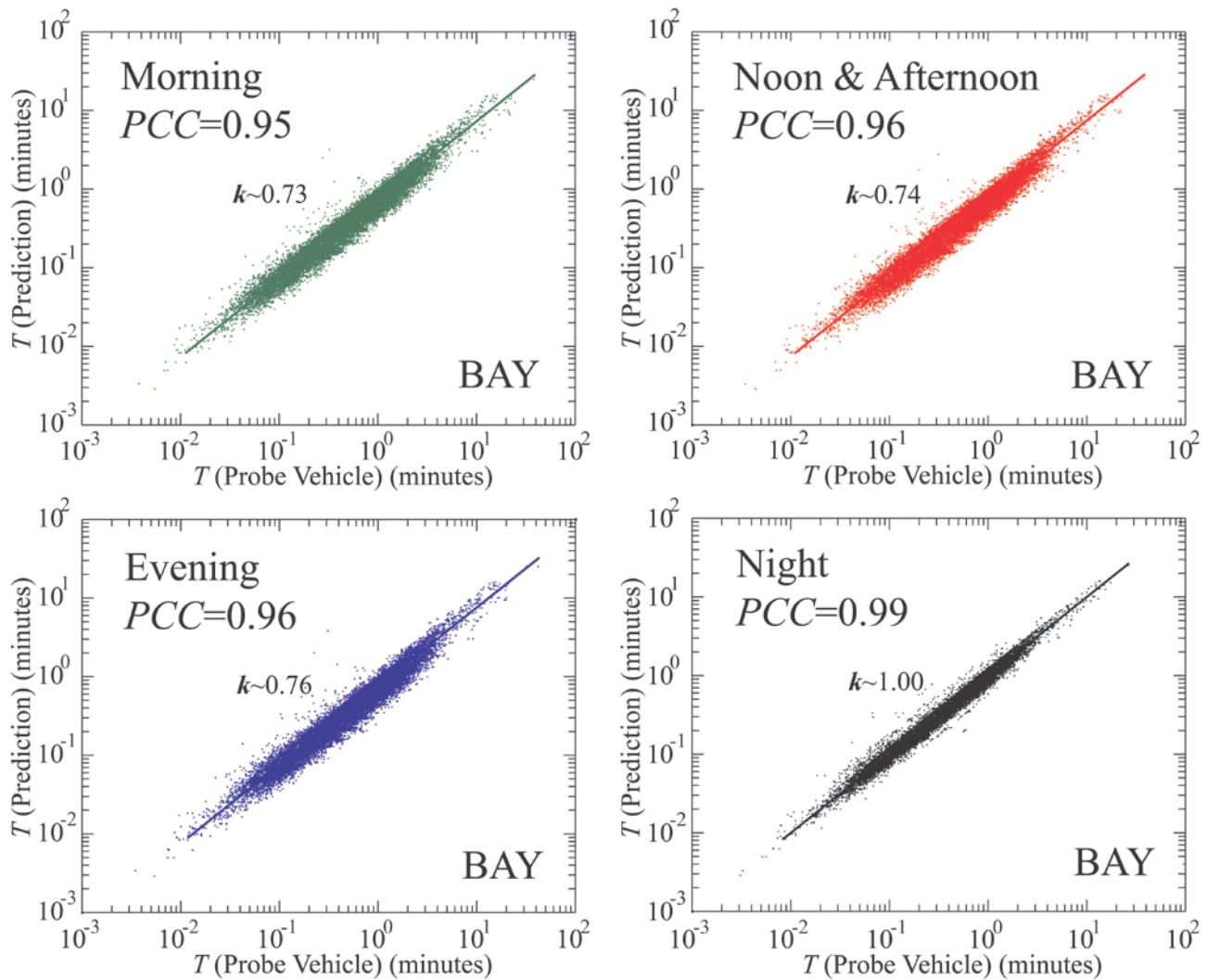


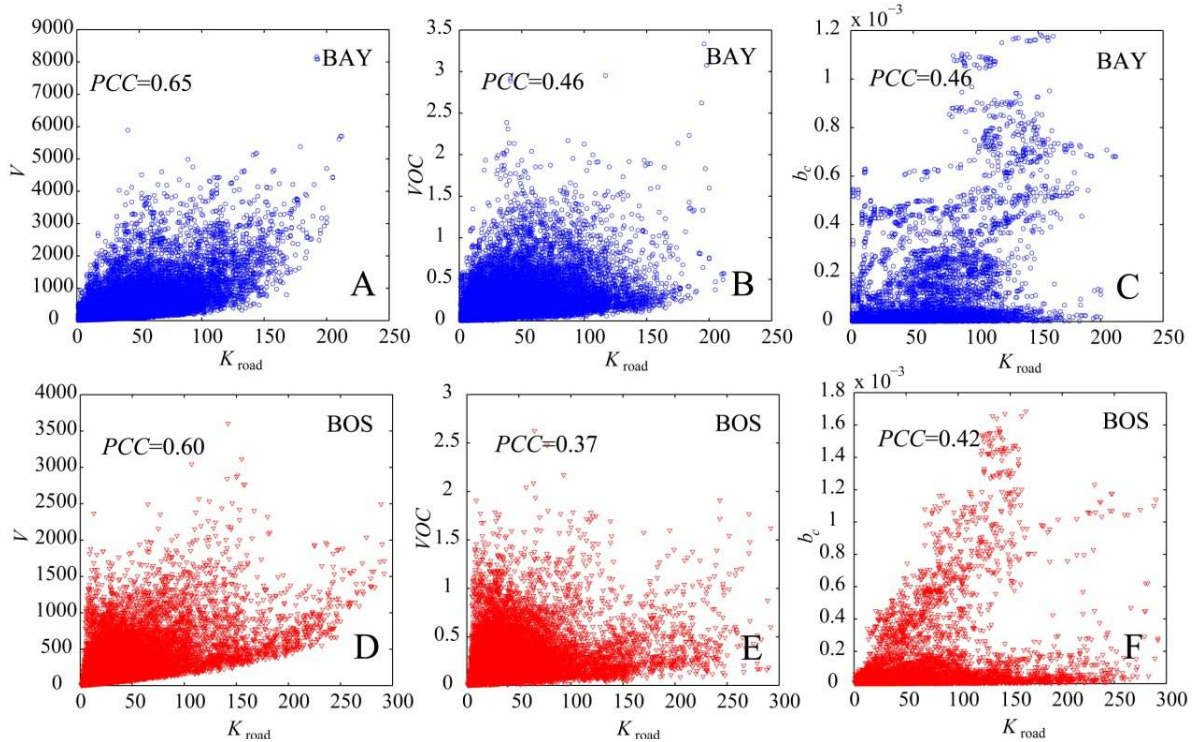
**Figure S14.** The predicted travel time is validated by the travel time estimated from the probe vehicle GPS data. Because traffic flow data is not available on arterial roads, the only available comparison variable to assess the validity of the method is travel time (which can be measured directly from probe data). To this day, this is the only feasible method to perform this comparison at a global scale and represents the latest state of the art.

### III. RESULTS

#### A. Supplementary Results

##### 1. *The road segment's degree is lowly correlated with traditional measures:*

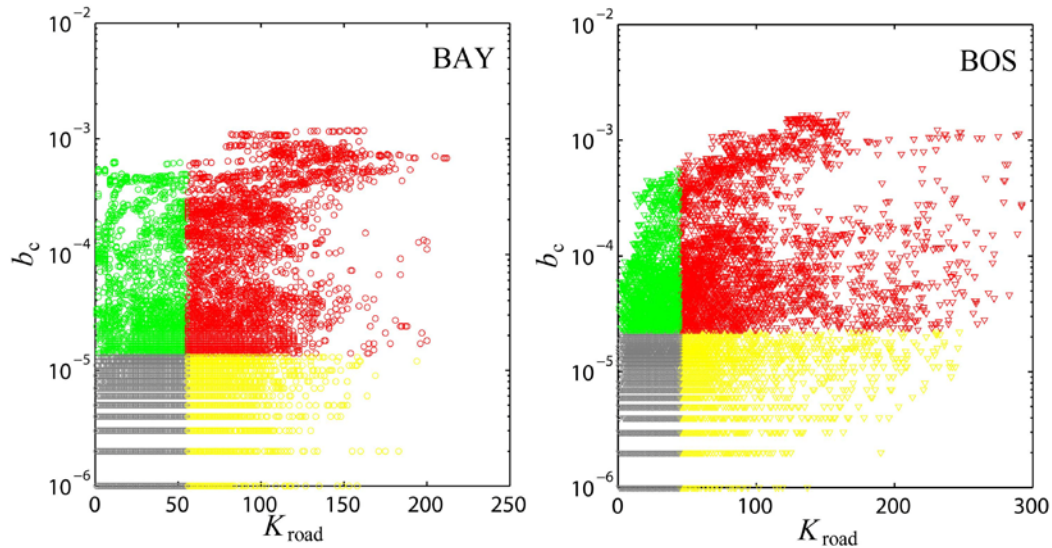
As Fig. S15 shows, although relatively large Pearson correlation coefficient  $PCC=0.65$  (BAY) and  $PCC=0.60$  (BOS) are measured, road segments with similar traffic flow can still have large difference in their  $K_{road}$ . We also find road segments with similar  $VOC$  can have very different  $K_{road}$  ( $PCC=0.46$  and  $PCC=0.37$  for the Bay Area and the Boston Area respectively). This result indicates that for road segments with similar condition of congestion, the diversity of their driver sources may be very different. The betweenness centrality  $b_c$  of a road determines its ability to provide a path between separated regions of the network. We find  $b_c$  also has low correlations with  $K_{road}$  (Fig. S15C and F).



**Figure S15.** Road segment's degree  $K_{road}$  has low correlations with its traffic flow  $V$ ,  $VOC$  and betweenness centrality  $b_c$ . (A) Pearson correlation coefficient ( $PCC$ ) between  $V$  and  $K_{road}$  in the Bay Area. (B)  $PCC$  between  $VOC$  and  $K_{road}$  in the Bay Area. (C)  $PCC$  between  $b_c$  and  $K_{road}$  in the Bay Area. (D), (E), (F) Same as (A), (B), (C) respectively but for the Boston Area.

## 2. Grouping the road segments according to their $b_c$ and $K_{road}$ :

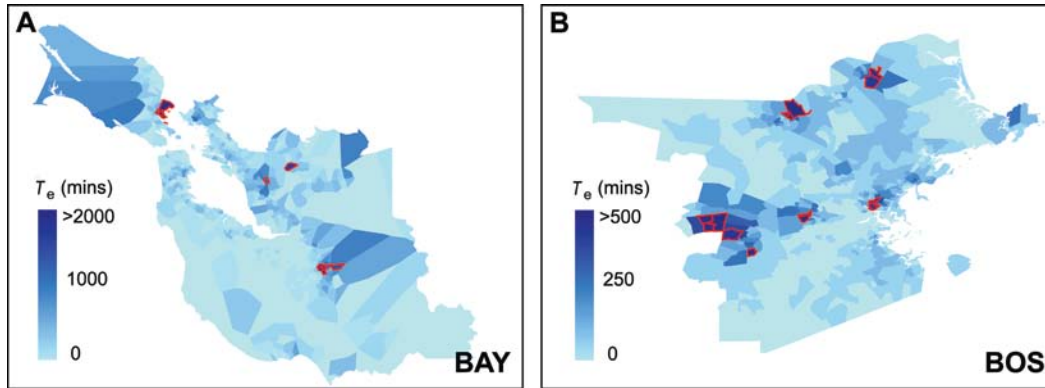
Fig. S16 shows the betweenness centrality  $b_c$  and the degree  $K_{road}$  of road segments. Road segments are grouped and depicted in different colors.



**Figure S16.** Types of roads defined by  $b_c$  and  $K_{road}$ . The road segments are grouped by their betweenness centrality  $b_c$  and degree  $K_{road}$ . The red symbols represent the roads with the largest 25% of  $b_c$  and  $K_{road}$ . The green symbols represent those with the largest 25% of  $b_c$  and the smallest 75% of  $K_{road}$ . The yellow symbols are those with the smallest 75% of  $b_c$  and the largest 25%  $K_{road}$ . The road segments depicted in grey have the smallest 75% of  $b_c$  and  $K_{road}$ .

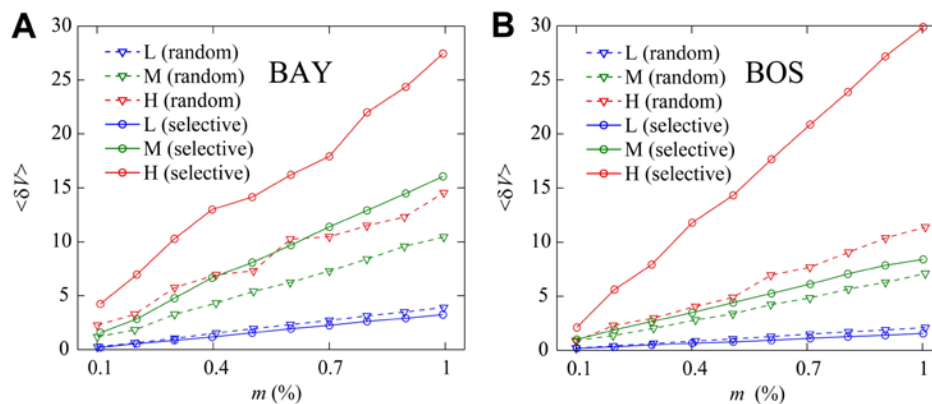
## 3. The total additional travel time $T_e$ in driver sources:

Fig. S17 shows the total additional travel time  $T_e$  of the driver sources. Due to the heterogeneity of road usage,  $T_e$  is very unevenly distributed in space in the two metropolitan areas, enabling us to easily locate the driver sources with high  $T_e$ . For the Bay Area, the top 1.5% driver sources (12 sources) with the largest  $T_e$  are selected. In the case study for the Boston Area, we select 15 driver sources (top 2%) with highest  $T_e$ . This selection makes sure that for a similar local trip reduction  $f$ , the global trip reduction  $m$  is same as that of the Bay Area.



**Figure S17.** (A) The total additional travel time  $T_e$  for each Bay Area driver source. The red polygons locate the pinpointed driver sources with  $T_e > 1,355$  minutes. Thus the drivers suffering from heavy traffic congestion are located. (B) Same as (A) but for the Boston Area. The red polygons locate the targeted 15 driver sources (top 2%) with a total of more than 400 minutes additional travel time in one hour of the morning commute.

To address the underlying reasons for the high efficiency of the selective strategy (Fig. 4B), we measure the average traffic flow reduction  $\delta V$  for road segments with different levels of  $VOC$ . As Fig. S18 shows, the red, green and blue curves correspond to the road segments with  $VOC > 1$  (High  $VOC$ ),  $0.5 < VOC \leq 1$  (Middle  $VOC$ ) and  $VOC \leq 0.5$  (Low  $VOC$ ) respectively. We find that for high  $VOC$  road segments,  $\delta V$  is much larger in a selective strategy for both Bay Area and Boston Area, indicating that the selective strategy can more efficiently decrease the traffic flows in the congested road segments.



**Figure S18.** (A) The average traffic flow reduction  $\langle \delta V \rangle$  over road segments with different  $VOC$  in the Bay Area. Red, green and blue symbols correspond to road segments with  $VOC > 1$ ,  $0.5 < VOC \leq 1$  and  $VOC \leq 0.5$  respectively. (B) Same as (A) but for the Boston Area.



#### 4. The results for other time periods:

Fig. S19 are counterpart figures for Fig. 1 and Fig. 2. It shows the corresponding results in the other three periods (Noon & Afternoon, Evening and Night). We find that the results for the three daytime periods show high similarities, whereas the results in the Night period are different due to minor road usage. These results indicate that using our modelling framework, we can capture the road usage pattern dynamically.

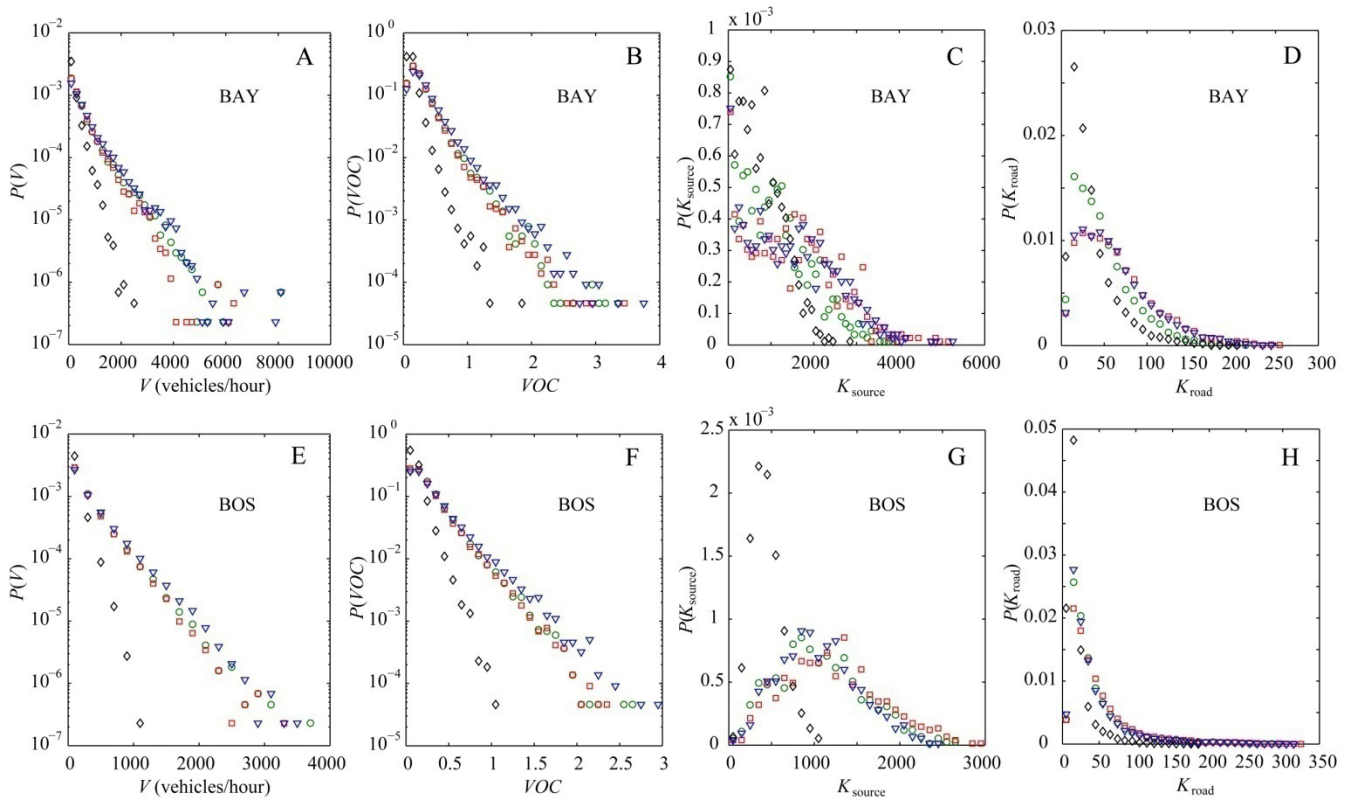


**Figure S19.** Green circles represent the results in Morning period, red squares represent the results in Noon & Afternoon period, blue triangulations represent the results in Evening period and black diamonds represent the results in Night period. (A) Distribution of the Bay Area one-hour traffic flow in the four time periods. The one-hour traffic flow in the Night period is much smaller than that found in the daytime periods. (B) Distribution of the Bay Area  $VOC$  in the four time periods. (C) Degree distributions of the Bay Area driver sources in the four time periods. (D) Degree distributions of the Bay Area road segments in the four time periods. (E), (F), (G), (H) are same as (A), (B), (C), (D) respectively but for the Boston Area.

### 5. The distance from road segment to its MDS:

We measure the distance  $d$  from each road segment to its major driver sources. We find that  $d$  can be well approximated by a log-normal distribution  $P(d) \sim e^{-(\ln(d)-\mu)^2/2\sigma^2}/(\sqrt{2\pi}\sigma d)$ . As Fig. S20 shows, the distance  $d$  centers around 4km and 7km for Bay Area and Boston Area respectively, indicating that the MDS are geographically nearby the corresponding road segment. However, there exist MDS that are far away from the road segment ( $>50$ km). The prediction of these specific MDS is beyond a traditional distance decaying function, and this is the power of our modeling framework in capturing the urban travel demand.

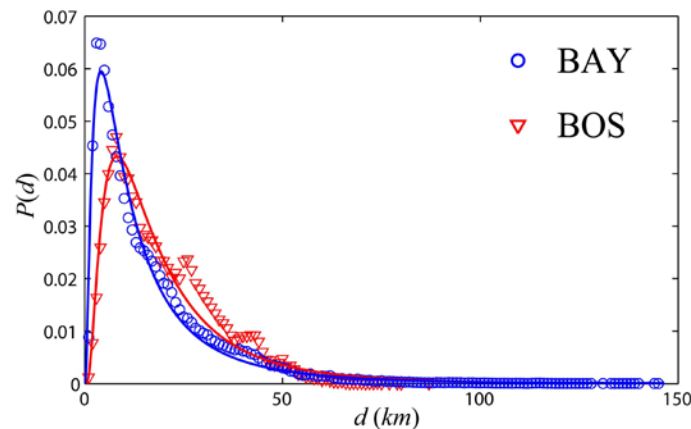


**Figure S20.** The distribution of the distance  $d$  from each road segment to its MDS. The blue circles represent the result for Bay Area and the red triangles represent the result for Boston Area. The distance  $d$  from each road segment to its MDS can be well approximated by a log-normal distribution  $P(d) \sim e^{-(\ln(d)-\mu)^2/2\sigma^2}/(\sqrt{2\pi}\sigma d)$  with  $\mu = 2.40$  (2.76),  $\sigma = 0.99$  (0.81),  $R^2=0.98$  (0.96) for Bay Area (Boston Area).

## B. Statistical Analysis

The purpose of this section is to support our findings with rigorous goodness-of-fit analysis. We evaluate goodness-of-fit statistics for parametric models in the paper by calculating the sum of squares due to error (SSE), the  $R^2$  and the root mean squared error (RMSE).

Area	$p_A$	$p_H$	$\beta_H$	$c_A$	$\alpha_A$	$R^2$	SSE	RMSE
BAY	0.876	0.124	0.00026	4.625e-008	2.43	0.991	5.38e+006	227.4
BOS	0.942	0.058	0.00046	2.581e-005	1.86	0.996	2.76e+006	135.8

**Table S2.** The distribution of betweenness centrality:  $P(b_c) = p_H \beta_H e^{-b_c/\beta_H} + p_A c_A b_c^{-\alpha_A}$ .  $p_A$  is the fraction of arterial roads,  $p_H$  is the fraction of highways,  $\beta_H$  is the average highway betweenness centrality,  $c_A$  and  $\alpha_A$  are estimated by the Matlab fitting toolbox.

Area	$p_A$	$p_H$	$v_A$	$v_H$	$R^2$	SSE	RMSE
BAY	0.876	0.124	373	1493	0.999	4.126e-009	1.193e-005
BOS	0.942	0.058	236	689	0.997	2.508e-008	3.959e-005

**Table S3.** The distribution of one-hour traffic flow:  $P(V) = p_A v_A e^{-V/v_A} + p_H v_H e^{-V/v_H}$ .  $p_A$  is the fraction of arterial roads,  $p_H$  is the fraction of highways,  $v_A$  is average traffic flow for arterial roads,  $v_H$  is the average traffic flow for highways.

Area	$\gamma$	$R^2$	SSE	RMSE
BAY	0.28	0.983	0.2199	0.08861
BOS	0.28	0.982	0.1769	0.08769

**Table S4.** The distribution followed by  $VOC$ :  $P(VOC) = \gamma e^{-VOC/\gamma}$ ,  $\gamma$  is the mean of  $VOC$ .

Area	$\tau$	$R^2$	SSE	RMSE
BAY	204.2	0.972	2.362e-006	0.000198
BOS	113.2	0.735	6.038e-005	0.001374

**Table S5.** The distribution followed by total additional travel time:  $P(T_e) = \tau e^{-T_e/\tau}$ ,  $\tau$  is the mean of  $T_e$ .

Area	$\mu_{\text{source}}$	$\sigma_{\text{source}}$	$R^2$	SSE	RMSE
BAY	1035.9	792.2	0.785	2.847e-007	8.893e-005
BOS	1017.7	512.3	0.914	1.540e-007	7.849e-005

**Table S6.** The statistical fits of driver source's degree:  $P(K_{\text{source}}) = e^{-(K_{\text{source}} - \mu_{\text{source}})^2 / 2\sigma_{\text{source}}^2} / (\sqrt{2\pi}\sigma_{\text{source}})$ , where  $\mu_{\text{source}}$  is the mean of  $K_{\text{source}}$  and  $\sigma_{\text{source}}^2$  is the variance.

Area	$\mu_{\text{road}}$	$\sigma_{\text{road}}$	$R^2$	SSE	RMSE
BAY	3.713	0.821	0.978	9.013e-006	0.0008326
BOS	3.359	0.724	0.989	1.271e-005	0.0006737

**Table S7.** The statistical fits of road segment's degree:

$$P(K_{\text{road}}) = e^{-(\ln(K_{\text{road}}) - \mu_{\text{road}})^2 / 2\sigma_{\text{road}}^2} / (\sqrt{2\pi}\sigma_{\text{road}} K_{\text{road}})$$

Strategy	$k$	$b$ ( $b \sim 0$ )	$R^2$	SSE	RMSE
BAY (Random)	6.931e+005	-0.0020	0.9019	4.349e+006	737.3
BAY (Selective)	2.261e+006	-0.0010	0.9820	7.753e+006	984.4
BOS (Random)	2.300e+005	0.0015	0.9818	8.299e+004	101.9
BOS (Selective)	1.181e+006	-0.0001	0.9966	4.023e+005	224.3

**Table S8.** The total additional travel time reduction  $\delta T$  with the trip reduction percentage  $m$  in the cases of selective and random strategies:  $\delta T = k(m - b)$ .

Periods	$k$	$R^2$	SSE	RMSE
Morning	0.7277	0.9093	1701	0.3204
Noon & Afternoon	0.7416	0.9200	1496	0.3005
Evening	0.7567	0.9178	1541	0.3049
Night	0.9951	0.9724	516.3	0.1765

**Table S9.** The validation of predicted travel time by the estimated travel time from probe vehicles' GPS data:  $T_{\text{prediction}} = kT_{\text{probe vehicle}}$ .

## REFERENCES:

1. Fu, T., Yin, X. & Zhang, Y. Voronoi algorithm model and the realization of its program. *Computer Simulation* **23**, 89-91 (2006).
2. Song, C., Qu, Z., Blumm, N. & Barabási, A.-L. Limits of predictability in human mobility. *Science* **327**, 1018-1021 (2010).
3. Chicago metropolitan agency for planning. <http://www.cmap.illinois.gov/travel-tracker-survey>
4. Navteq official website. <http://www.navteq.com/>
5. Highway capacity manual 2000 (Transportation Research Board. December, 2000).
6. Villalobos, J. R. *et al.* Logistics capacity study of the guaymas-tucson corridor (A report to the Arizona Department of Transportation, 2005).
7. Barthélemy, M. Spatial networks. *Physics Reports* **499**, 1–101 (2011).
8. Herrera, J. C. *et al.* Dynamic estimation of OD matrices for freeways and arterials. *Technical Report* (Institute for Transportation Studies, UC Berkeley, 2007).
9. Herrera, J. C. *et al.* Evaluation of traffic data obtained via GPS-enabled mobile phones: the mobile century field experiment. *Transportation Research C* **18**, 568-583 (2010).
10. Andrienko, G. *et al.* Visual cluster analysis of large collections of trajectories. *IEEE Visual Analytics Science and Technology* (2009).
11. Calabrese, F., Lorenzo, G. D., Liu, L. & Ratti, C. Estimating origin-destination flows using opportunistically collected mobile phone location data from one million users in Boston metropolitan area. *IEEE Pervasive Computing*, October-December, 36-44 (2011).
12. Candia, J. *et al.* Uncovering individual and collective human dynamics from mobile phone records. *J. Phys. A* **41**, 224015 (2008).
13. State averages for private vehicle occupancy, carpool size and vehicles per 100 workers. <http://www.nctr.usf.edu/clearinghouse/censusavo.htm>
14. National household travel survey daily travel quick facts. [http://www.bts.gov/programs/national\\_household\\_travel\\_survey/daily\\_travel.html](http://www.bts.gov/programs/national_household_travel_survey/daily_travel.html)
15. Seto, Y. W., Holt, A., Rivard, T. & Bhatia, R. Spatial distribution of traffic induced noise exposures in a US city: an analytic tool for assessing the health impacts of urban planning decisions. *International Journal of Health Geographics* **6**, 24 (2007).
16. Dijkstra, E. W. A note on two problems in connexion with graphs. *NumerischeMathematik* **1**, 269–271 (1959).

17. Chen, M. & Alfa, A. S. A Network design algorithm using a stochastic incremental traffic assignment approach. *Transportation Science* **25**, 215-224 (1991).
18. Travel demand modeling with TransCAD 5.0, user's guide (Caliper, 2008).
19. Eash, E. W., Janson, B. N. & Boyce, D. E. Equilibrium trip assignment: advantages and implications for practice. *Transportation Research Record* **728**, 1-8 (1979).
20. Work, D. B. *et al.* A traffic model for velocity data assimilation. *Appl. Math. Res. Express* **1**, 1-35 (2010).
21. Hoh, B. *et al.* Virtual trip lines for distributed privacy preserving traffic monitoring. *Proceedings of the 6th international conference on Mobile systems, applications, and services Mobile Systems and Applications*, Breckenridge, June 17-18 (2008).